Crucial roles of *Foxa2* in mouse anterior–posterior axis polarization via regulation of anterior visceral endoderm-specific genes

Chiharu Kimura-Yoshida*†, E. Tian‡, Hiroshi Nakano*†, Saori Amazaki*, Kayo Shimokawa*, Janet Rossant§, Shinichi Aizawa¶, and Isao Matsuo*†‖

*Department of Molecular Embryology, Osaka Medical Center and Research Institute for Maternal and Child Health, Osaka Prefectural Hospital Organization, Murodo-cho, Izumi, Osaka 594-1101, Japan; †Head Organizer Project, Vertebrate Body Plan Group, RIKEN Center for Developmental Biology (CDB), Kobe, Hyogo 650-0047, Japan; ‡Department of Morphogenesis, Institute of Molecular Embryology and Genetics, Kumamoto University, Kumamoto 860-0811, Japan; §Program in Developmental Biology, Hospital for Sick Children, 555 University Avenue, Toronto, ON, Canada M5G 1X8; and ¶Vertebrate Body Plan Group, RIKEN CDB, Kobe, Hyogo 650-0047, Japan

Edited by Kathryn V. Anderson, Sloan–Kettering Institute, New York, NY, and approved February 16, 2007 (received for review September 6, 2006)

Anterior visceral endoderm (AVE) plays essential roles with respect to anterior–posterior axis development in the early mouse embryo. To assess the genetic cascade involved in AVE formation, the cis-regulatory elements directing expression of vertebrate *Otx2* genes in the AVE were analyzed via generation of transgenic mice. *Otx2* expression in AVE is regulated directly by the forkhead transcription factor, *Foxa2*. Moreover, *Foxa2* is essential for expression of the *Wnt* antagonists, *Dkk1* and *Cerl*, in visceral endoderm during the pre- to early streak stages; however, *Foxa2* appears to be dispensable for subsequent *Dkk1* expression associated with forebrain induction. Thus, we propose that *Foxa2* is crucial in early anterior–posterior axis polarization in terms of regulation of expression of AVE-specific genes. These findings provide profound insights into conserved roles of *Foxa2* transcription factors in anterior specification throughout the evolution of the chordate body plan.

cis element | gene regulation | Wnt signaling | forebrain induction | *Dkk1*

The initial anterior–posterior (A–P) axis in mouse embryos is established before gastrulation (1). By embryonic day (E)5.5, the mouse embryo proper, consisting of epiblast and visceral endoderm (VE), develops a clear proximal–distal axis, as marked by expression of *Hex* in the distal VE (DVE). By E6.0, DVE cells have migrated directionally to the prospective anterior side, and the proximal markers (*Cripto*, *Wnt3*, and *Nodal*) have shifted to the posterior side where primitive streak formation will occur. Several lines of evidence have indicated that the anterior visceral endoderm (AVE) is required for normal anterior patterning (2, 3). Notably, this function depends on the production of *Nodal* and *Wnt* antagonists, such as *Cerl*, *Lefty1*, and *Dkk1*, which locally repress the posteriorizing effects of Nodal and Wnt signals (4–6). Moreover, these antagonists also regulate migration of DVE cells toward the prospective anterior side (7–9). However, little is known regarding the genetic cascade governing AVE formation, i.e., how transcription factors control antagonists and one another in AVE cells in a spatially and temporally specific manner.

The *Otx2* gene, a paired-like class homeobox gene, plays critical roles in the generation and function of AVE (10). *Otx2* is expressed in the DVE at E5.5 and subsequently in the AVE. In the absence of *Otx2*, DVE cells fail to migrate toward the anterior. Consistent with this observation, *Dkk1* is not activated in *Otx2* mutant VE; consequently, canonical Wnt signaling is up-regulated (8). The current investigation determined that a cis-regulatory element highly conserved among vertebrates is essential for *Otx2* expression in AVE. Biochemical and genetic analysis revealed that *Foxa2* (previously named *Hnf3β*), a forkhead family transcription factor, directly transactivates *Otx2* expression. More importantly, *Foxa2* is necessary for expression of AVE-specific genes including *Wnt* antagonists in A–P axis polarization.

Results and Discussion

Identification of the Crucial Core Cis Element for Vertebrate Otx2 Expression in AVE. A 5′ 1.8-kb mouse *Otx2* promoter region directs expression in the DVE at E5.5 and in the AVE from the pre- to the midstreak stages (11). To identify the specific cis elements necessary for AVE expression in this region, a series of deletion constructs was generated and tested for activity in transgenic mice (Fig. 1*A*, #1–6). The activity was unaffected by the deletion of −683 to −594 bp (Fig. 1 *A* and *B*, #1–3); however, removal of an additional 51 bp (to −543 bp) abolished reporter activity in AVE (Fig. 1*C*, #4). Consistently, internal excision of the 51-bp fragment from the 1.8-kb promoter led to complete loss of expression of the transgene (Fig. 1*E*, #8). However, deletion of −648 to −594 bp did not affect activity (Fig. 1*D*, #7). These deletion analyses determined that the crucial element for induction of mouse *Otx2* expression in AVE consists of 51 nucleotides (from −594 to −543 bp).

Alignment of the sequence with the corresponding regions from human and chick *Otx2* promoters identified a 51-bp stretch characterized by 100% and 90.2% identity, respectively [supporting information (SI) Fig. 5*A*]. Examination of the reporter activity of the human and chick promoters revealed that these conserved 51-bp segments are also crucial for AVE expression (SI Fig. 5). These findings in concert strongly support the critical nature of the 51-bp sequence with respect to cis activity in AVE.

Comparison of the sequences of different species appears to afford a powerful approach with respect to identification of functional segments for gene regulation (12). Thus, we exploited the compact genome of the pufferfish, *Takifugu rubripes* (*Fugu*), which is approximately eight times smaller than the mouse genome (13). More importantly, the nucleotide sequence between mouse and pufferfish genomes in the noncoding region displays a higher degree of divergence relative to that of human or chick genomes (14). Cis activity of the *Fugu Otx2* genomic

Author contributions: C.K.-Y., J.R., S. Aizawa, and I.M. designed research; C.K.-Y., E.T., H.N., S. Amazaki, K.S., and I.M. performed research; H.N., J.R., and S. Aizawa contributed new reagents/analytic tools; C.K.-Y. and I.M. analyzed data; and C.K.-Y., J.R., S. Aizawa, and I.M. wrote the paper.

The authors declare no conflict of interest.

This article is a PNAS Direct Submission.

Abbreviations: A–P, anterior–posterior; E*n*, embryonic day *n*; VE, visceral endoderm; DVE, distal VE; AVE, anterior VE.

‖To whom correspondence should be addressed. E-mail: imatsuo@mch.pref.osaka.jp.

This article contains supporting information online at www.pnas.org/cgi/content/full/0607779104/DC1.

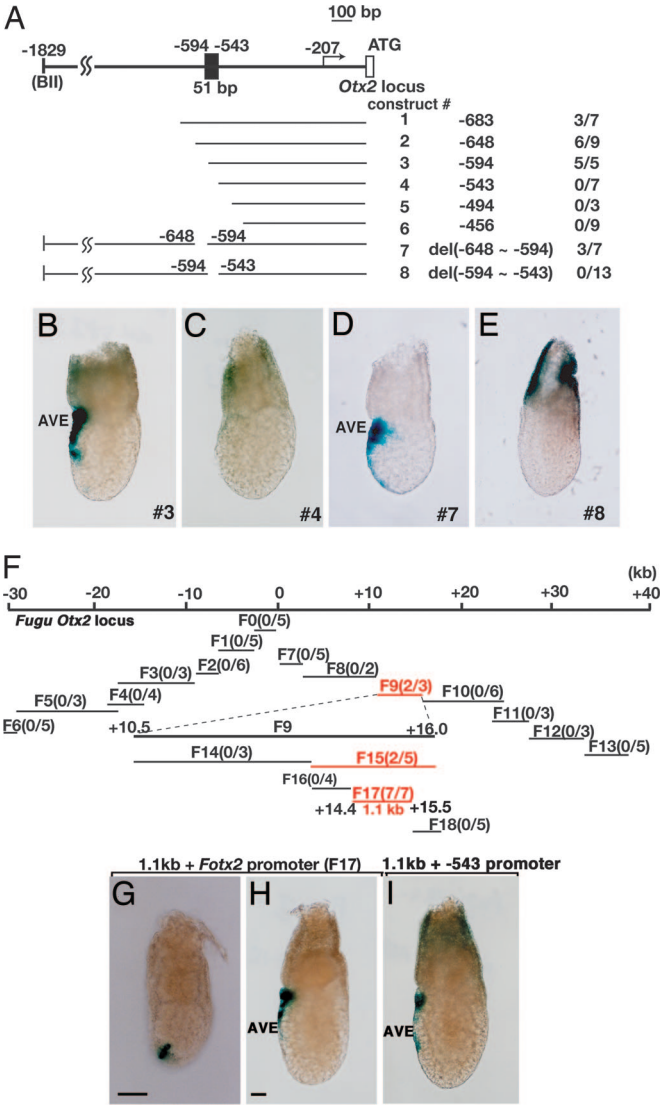

Fig. 1. Identification of crucial cis elements in mouse and *Fugu Otx2* genes. (*A*) The *Otx2* promoter region appears at the top; below the promoter region, the mutant constructs linked to a *lacZ* reporter gene at the translational start site for expression analysis are listed. The filled box indicates the 51-bp region. Transcription is initiated at −207 bp (34). Construct numbers are noted on the left. The number of *lacZ*-positive embryos in the AVE among transgenic embryos is indicated on the right. (*B–E*) Lateral views of E6.5 transgenic embryos after β-gal staining. (*F*) Schematic diagram of the *lacZ*-transgene constructs throughout the *Fugu Otx2* locus. F9, F15, and F17 constructs display *lacZ* activity in AVE. The number of *lacZ*-positive embryos in the AVE among transgenic embryos is displayed in parentheses to the right of each construct number. (*G–I*) X-Gal staining patterns of representative transgenic embryos at E5.75 (*G*) and E6.5 (*H* and *I*). (Scale bars: 50 μm.)

fragments (from −30.5 to +38.5 kb), which directs expression in the AVE, was surveyed via production of transgenic mouse lines (Fig. 1*F*) (14). Consequently, cis activity in the AVE was detected in the 5-kb fragment (from +10.5 to +15.5 kb) (Fig. 1*F*, F9). Further subdivision of the 5-kb fragment mapped this activity to a 1.1-kb fragment (from +14.4 to +15.5 kb) (Fig. 1 *G* and *H*, F17). Moreover, the 1.1-kb fragment, fused with a heterologous promoter, namely, the mouse *Otx2* minimal promoter from −543 bp (#4), could drive AVE-specific expression (Fig. 1*I*). This observation indicated that the *Fugu* 1.1-kb fragment possesses cis activity similar to that of the mouse 51-bp sequence.

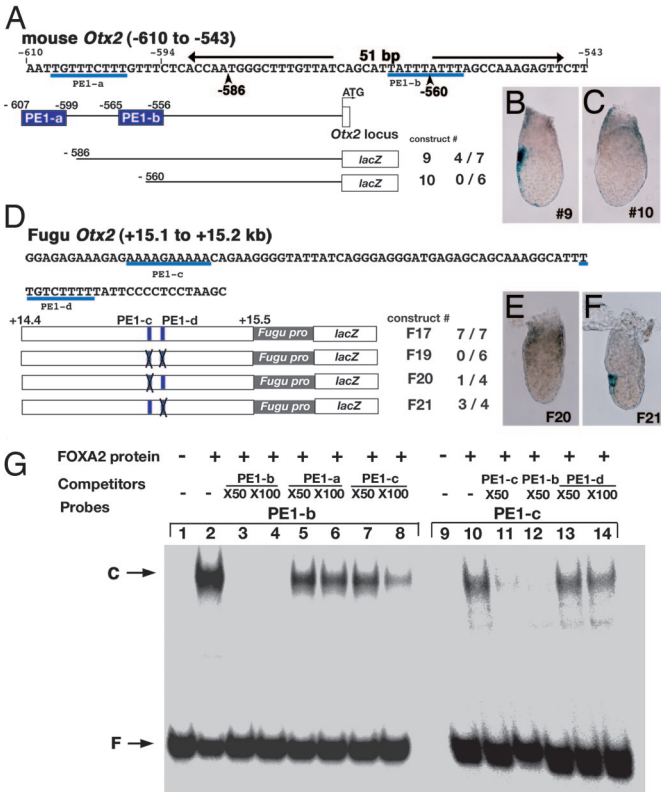

Fig. 2. Identification of *Foxa2* binding sites that were conserved between mouse and *Fugu Otx2* genes. (*A*) Nucleotide sequences of mouse *Otx2* 5′-upstream region and schematic diagram of the transgene constructs. (*D*) Nucleotide sequence within the *Fugu* genomic sequence and schematic diagram of the transgene constructs. (*B*, *C*, *E*, and *F*) Lateral views of E6.5 transgenic embryos after β-gal staining. (*G*) EMSA. FOXA2 protein and labeled DNA probes (PE1-b and PE1-c) formed a complex, which is indicated with the arrow labeled "C." The arrow labeled "F" indicates unbound labeled oligonucleotides.

A search was conducted for conserved motifs between the mouse 51-bp and the *Fugu* 1.1-kb sequences to identify a crucial core cis element in terms of possible transcriptional factor binding sites; as a result, one AT-rich element, TNTTTNTTT (referred to as PE1), emerged (Fig. 2 *A* and *D*). The mouse *Otx2* promoter possesses two PE1 sites (PE1-a and PE1-b); PE1-a is located outside the 51-bp fragment, whereas PE1-b occurs within the 51-bp stretch (Fig. 2*A*). To establish whether the PE1 elements are necessary for cis-regulatory activity, additional expression analysis was performed involving precise mutant constructs (Fig. 2*A*). A 5′ deletion construct from −586 bp to the translational start site, which contained one PE1 element, continued to direct *lacZ* expression in the AVE (Fig. 2*B*, #9). However, a second deletion construct, which lacked the PE1-b element, displayed no cis activity (Fig. 2*C*, #10). The pufferfish 1.1-kb fragment, which drives AVE expression, contains two PE1 sequences (Fig. 2*D*, F17); mutant constructs, which exhibited mutations in one or both PE1 elements (F19–21), were examined for cis activity (Fig. 2 *D–F*). Mutation of both PE1 sites resulted in complete loss of expression; moreover, AVE expression was more greatly reduced by the PE1-c mutation than by the PE1-d mutation (Fig. 2 *D–F*, F19–21). Consequently, the PE1-c site is more critical with respect to AVE expression in comparison to the PE1-d site in the *Fugu* transgene. These data clearly demonstrated that both mouse and *Fugu* PE1 elements are essential for cis activity in AVE.

Foxa2 Directly Controls Otx2 Expression in AVE. A search for transcription factor binding motifs related to PE1 revealed that the

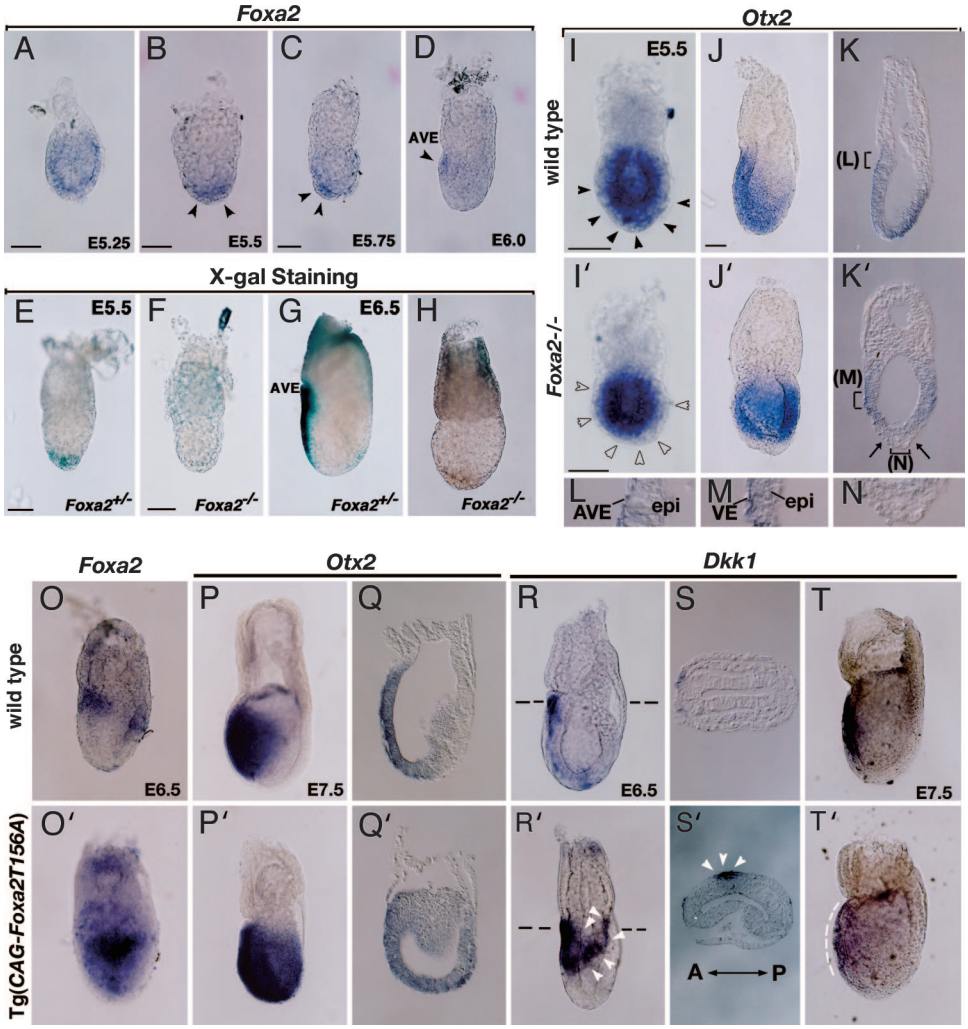

Fig. 3. *Foxa2* regulates *Otx2* expression in AVE via the PE1 element. (*A–D*) *Foxa2* mRNA expression was assessed after implantation to the prestreak stage by using whole-mount *in situ* hybridization. (*E–H*) X-Gal staining at E5.5 (*E* and *F*) and E6.5 (*G* and *H*). Lateral views of embryos carrying transgene #3 in the *Foxa2*$^{+/-}$ (*E* and *G*) and *Foxa2*$^{-/-}$ (*F* and *H*) backgrounds are shown. (*I–T*) Whole-mount *in situ* hybridization of *Otx2* in the wild-type (*I* and *J*) and *Foxa2*$^{-/-}$ mutant (*I*′ and *J*′) embryos and the corresponding sagittal sections (*K* and *K*′) are shown. *Otx2* expression is absent in the entire VE at E5.5; in contrast, *Otx2* expression is evident in the epiblast at E5.5 (*I* and *I*′, filled and open arrowheads). *Otx2* expression, which is absent in the DVE, is present in the epiblast and proximal VE (*J*′, arrows in *K*′, and *L–N*) at E6.5. The morphological structure of *Foxa2*$^{-/-}$ DVE, which displays aberrant thickening, is consistent with that observed in *Otx2*$^{-/-}$ embryos (*K*′, arrows, and *N*) (11). *Foxa2*, *Otx2*, and *Dkk1* mRNA expression in wild-type (*O–T*) and Tg (*CAG-Foxa2T156A*) (*O*′*–T*′) embryos and the corresponding sagittal (*Q* and *Q*′) and transverse (*S* and *S*′) sections are shown. Ectopic *Dkk1* expression is apparent in the posterior aspect of the transgenic VE at E6.5 (*R*′ and *S*′, white arrowheads). A, anterior; P, posterior. (Scale bars: 50 μm.)

consensus recognition sequence of *Foxa2*, KGNATRTT-TRYTTW, matches the PE1 sites (http://motif.genome.ad.jp/). *Foxa2* expression in the VE has been shown to play crucial roles in A–P axis development, although the mechanism has not been clarified (15, 16). Therefore, the ability of *Foxa2* to regulate directly *Otx2* expression in AVE through the PE1 element was examined (Figs. 2*G*, 3, and 4). EMSA employing FOXA2 protein synthesized *in vitro* was performed to determine whether FOXA2 binds directly to the PE1 sequences (Fig. 2*G*). Precise EMSA experiments involving PE1 oligonucleotides demonstrated that FOXA2 protein can bind directly to PE1-b and PE1-c *in vitro* (Fig. 2*G*). The lower affinity of the PE1-a and PE1-d sites for FOXA2 is consistent with our expression analysis of mutant constructs (Fig. 1*D* and Fig. 2 *A–F*).

Endogenous *Foxa2* mRNA expression was analyzed by using whole-mount *in situ* hybridization to assess whether *Foxa2* expression coincides with *Otx2* expression within the VE (Fig. 3 *A–D*). *Foxa2* expression was apparent in the embryonic portion of the VE before E5.5 as reported (Fig. 3*A*) (17). *Foxa2* expression was restricted to the DVE around E5.5 (Fig. 3*B*); furthermore, *Foxa2* was expressed asymmetrically in the prospective anterior aspect of the VE at E5.75 and E6.0 (Fig. 3 *C* and *D*). These findings demonstrated that *Foxa2* expression is identical to *Otx2* expression in VE from E5.5 to E6.0 (11).

Otx2-lacZ transgene activity in the *Foxa2* mutant background was analyzed to evaluate *Foxa2* participation in *Otx2* expression (Fig. 3 *E–H*). First, hemizygous transgenic mice carrying construct #3 (Fig. 1*B*) were crossed with *Foxa2*$^{+/-}$ mice (16), followed by examination of the cis activity in *Foxa2*$^{-/-}$ embryos. *LacZ* expression of transgene #3 was abolished by the *Foxa2* null mutation (Fig. 3 *F* and *H*). Additionally, endogenous *Otx2* transcripts were not detected within the VE of *Foxa2*$^{-/-}$ embryos as early as E5.5 (Fig. 3*I*′). At subsequent E6.5, *Otx2* expression, which were evident in the epiblast and proximal VE, were absent in the mutant DVE (Fig. 3*J*′, *K*′, and *L–N*). Next, transgenic mice carrying a constitutive active form of *Foxa2* cDNA under the control of the *CAG* promoter were

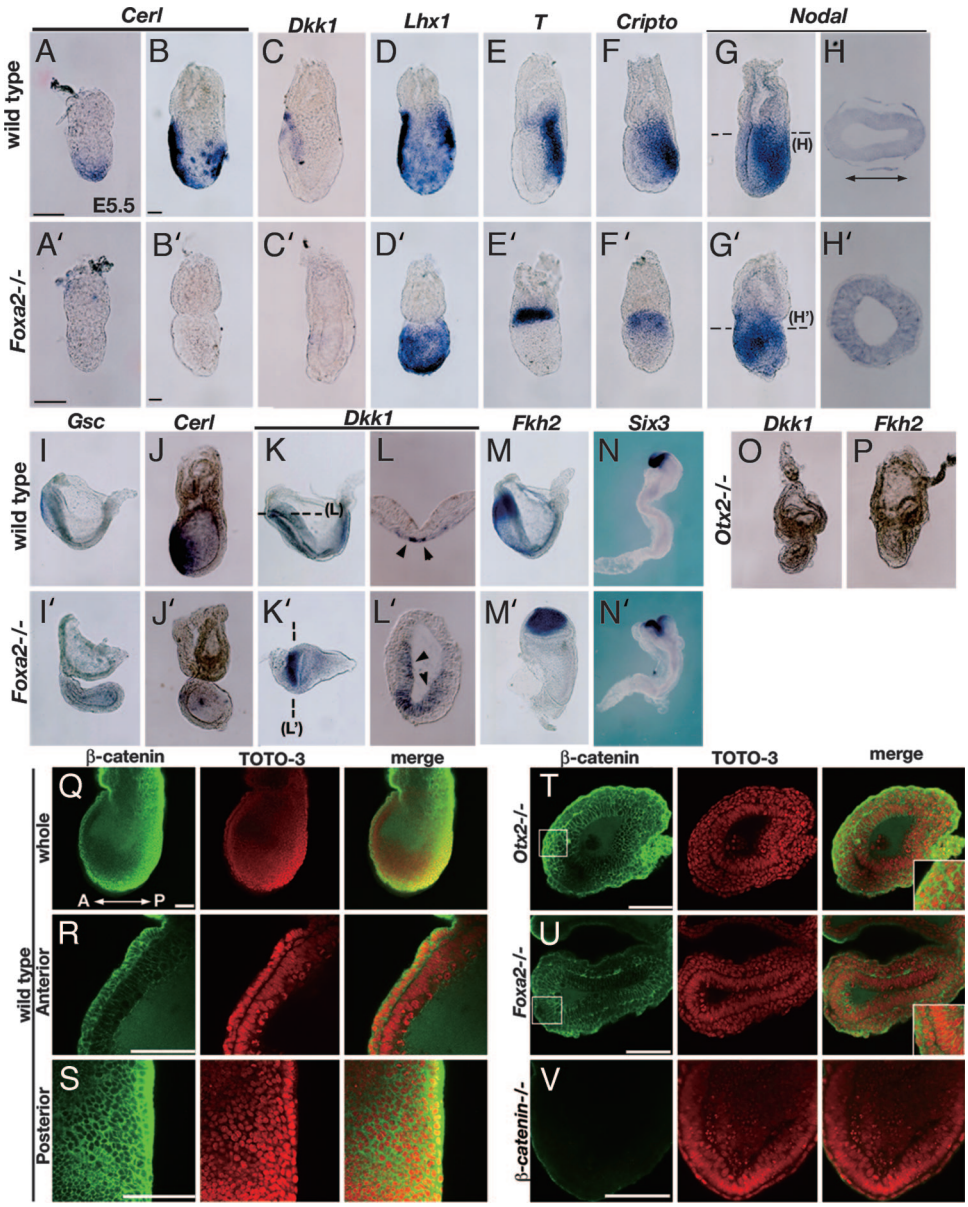

Fig. 4. A–P axis patterning is affected in *Foxa2*$^{-/-}$ embryos. Whole-mount *in situ* hybridization of wild-type (*A–N*), *Foxa2*$^{-/-}$ (*A′–N′*), and *Otx2*$^{-/-}$ mutant (*O* and *P*) embryos is shown. E5.5 (*A* and *A′*), E6.5 (*B–H* and *B′–H′*), E7.5 (*I--M*, *I′–M′*, *O*, and *P*), and E8.5 (*N* and *N′*) are shown; *Cerl* (*A*, *A′*, *B*, *B′*, *J*, and *J′*), *Dkk1* (*C*, *C′*, *K*, *K′*, *L*, *L′*, and *O*), *Lhx1* (*D* and *D′*), *T* (*E* and *E′*), *Cripto* (*F* and *F′*), *Nodal* (*G*, *G′*, *H*, and *H′*), *Gsc* (*I* and *I′*), *Fkh2* (*M*, *M′*, and *P*), and *Six3* (*N* and *N′*) are also shown. Lateral view of embryos (*G*, *G′*, *K*, and *K′*) and their transverse sections (*H*, *H′*, *L*, and *L′*), respectively, are shown. Expression of the active form of β-catenin protein at E7.5 is shown in *Q–V*. Fluorescent images of wild-type (*Q--S*), *Otx2*$^{-/-}$ (*T*), *Foxa2*$^{-/-}$ (*U*), and *β-catenin*$^{-/-}$ (*V*) embryos, respectively, are shown. Anti-active-β-catenin (green), TOTO-3 (nuclei, red), and the merged image are shown. (Scale bars: *A*, *A′*, *B*, and *B′*, 50 μm; *Q--V*, 100 μm.)

generated to assess whether *Foxa2* can transactivate *Otx2* expression (Fig. 3 *O′–Q′*). In the active form of *Foxa2*, a 156th-threonine, a phosphorylation target of *Akt* kinase, is mutated to alanine; consequently, dephosphorylated FOXA2 is exclusively localized in the nucleus (18). In the *Foxa2*-misexpressing embryos, *Otx2* expression was expanded to the posterior side beyond the endogenous domain at E7.5 (Fig. 3 *P′* and *Q′*). The aforementioned findings demonstrated that *Foxa2* mediates *Otx2* expression in AVE primarily through the PE1-b element.

Foxa2 Is Essential for Expression of Wnt Antagonists in AVE but Dispensable for Forebrain Induction. Expression of several molecular markers associated with A–P axis polarization were examined in *Foxa2*$^{-/-}$ embryos at E6.5 to E8.5 to determine whether *Foxa2* had broader roles in A–P axis development than just controlling *Otx2* expression (Fig. 4). Consequently, we found that *Foxa2*$^{-/-}$ embryos fail to express *Wnt* antagonists and thereby presumably to form the A–P axis correctly (Fig. 4 *A′–H′* and SI Fig. 6 *A–D′′*). Expression of *Cerl*, the *Nodal*, *Bmp*, and *Wnt* antagonist (5), was not observed in the *Foxa2*$^{-/-}$ embryo as early as E5.5 (Fig. 4 *A′* and B′). Additionally, expression of *Dkk1*, another *Wnt* antagonist, was absent or sharply reduced in *Foxa2*$^{-/-}$ embryos (Fig. 4*C′*). Consistent with these results, *Dkk1* expression was notably expanded in *Foxa2* (*T156A*) misexpressing embryos at E6.5 (Fig. 3 *R′* and *S′*). On the other hand, expression of *Lhx1* and *sFRP1*, which also mark the AVE of wild-type embryos, was detected in *Foxa2*$^{-/-}$ DVE (Fig. 4 *D* and *D′* and SI Fig. 6 *A–B′*). Expression of the posterior markers, *T*, *Cripto*, and *Nodal*, which was coordinated with that of AVE markers, was apparent in the proximal side of *Foxa2*$^{-/-}$ embryos at E6.5 (Fig. 4 *E′–H′*). Consistent with failure in DVE

migration, β-catenin expression was markedly up-regulated in the DVE of *Foxa2*$^{-/-}$ mutant embryos at E6.5 (C.K.-Y. and I.M., data not shown). These findings indicated that *Foxa2* is essential for DVE migration via regulation of the AVE-specific genes including *Wnt* antagonists.

Previous study with *Otx2* and *Foxa2* double mutant embryos suggests that both genes genetically interact in forebrain development at later E9.5 (19); however, precise interaction within the VE is poorly understood. Then, expression of *Dkk1* was examined in *Otx2*$^{+/-}$;*Foxa2*$^{+/-}$ double mutant embryos, and, consequently, *Dkk1* expression was reduced markedly in the AVE of *Otx2*$^{+/-}$;*Foxa2*$^{+/-}$ embryos; in contrast, *Cerl* expression was not reduced (SI Fig. 6 *E–G*). These data suggest that *Foxa2* and *Otx2* genes act cooperatively to induce *Dkk1* expression in AVE; additionally, these results indicate that *Foxa2* regulation of *Cerl* expression is largely independent of *Otx2*.

To determine more precisely whether *Foxa2* mediates A–P axis patterning outside the AVE, gene expression in *Foxa2*$^{-/-}$ embryos was examined at subsequent E7.5. *Gsc* and *Cerl* expressions were absent, which is probably attributable to failure in terms of proper formation of anterior mesendoderm (Fig. 4 *I′* and *J′*). However, *Dkk1* expression appeared to be up-regulated ectopically in the ectoderm of *Foxa2*$^{-/-}$ embryos at E7.5 (Fig. 4 *K′* and *L′*; $n = 7/9$). Consequently, *Foxa2*$^{-/-}$ embryos were able to form forebrain transiently marked by *Fkh2* ($n = 3/4$) and *Six3* ($n = 4/5$) expression (Fig. 4 *M′* and *N′*) (20), whereas *Otx2*$^{-/-}$ embryos fail to express *Dkk1*, *Fkh2*, and *Six3* (Fig. 4 *O* and *P*) (10). Because inhibition of canonical Wnt signaling is essential for forebrain induction (21–23), unexpected induction of *Dkk1* expression may account for the partial rescue of anterior development in *Foxa2*$^{-/-}$ embryos. *Dkk1* expression was reduced substantially in *Foxa2* (T156A) misexpressing embryos (Fig. 3*I′*), and misexpression of *Dkk1* cDNA led to anterior expansion in the mouse embryos (C.K.-Y. and I.M., data not shown), which are consistent with this hypothesis; moreover, expression of the active form of β-catenin was down-regulated in *Foxa2*$^{-/-}$ embryos in a manner similar to that of the wild-type embryo at E7.5, whereas β-catenin expression was markedly up-regulated in *Otx2*$^{-/-}$ embryos (Fig. 4 *Q–V*). These observations, in concert, indicated that *Foxa2* is essential for A–P axis polarization with respect to regulation of expression of multiple AVE-specific genes within the VE of pregastrula embryos; on the other hand, *Foxa2* appears to be dispensable for transient forebrain induction.

Finally, demonstration that pufferfish *Otx2* contains cis elements that can control AVE expression in transgenic mice (Figs. 1 and 2) suggests the possible presence of tissues equivalent in function to AVE in teleosts. Orthologues of *Foxa2* genes are expressed in the endoderm of all chordates examined before gastrulation (24, 25). Consistently, ascidian *Otx* expression is directly regulated by *FoxA-a*, an ascidian homologue of *Foxa2* (26–28). Moreover, ascidian *FoxA-a*, which is the earliest determinant of the ascidian anterior ectoderm, directly activates *Ci-sFRP1/5*, a canonical Wnt antagonist (27, 28). Thus, the genetic regulation of *Otx* and Wnt antagonists by *Foxa2* genes for anterior specification is highly conserved throughout the evolution of the chordate body plan.

Materials and Methods

Experimental Animals. Mouse *Otx2* promoter constructs (#1–6, 9, and 10) were produced via deletion of the 5′ flanking regions fused to the *lacZ* reporter, *VEcis-lacZ* (10). *Fugu* genomic constructs (F0–18) were generated as described (14). Internal deletion constructs (#7 and 8, F19–21) were generated by PCR-based mutagenesis. The *CAG-Foxa2 T156A* transgene construct was produced based on the method of Kimura-Yoshida *et al.* (8). Details regarding the construction of the transgene vectors are available upon request. Transgenic mice were produced via microinjection of fertilized eggs from CD-1 as described (29). Transgene integrations were identified by PCR analysis. β-catenin mutant mice (30) were obtained from The Jackson Laboratory (Bar Harbor, ME). Mice were housed under the guidelines of Osaka Medical Center and Research Institute for Maternal and Child Health for animal and recombinant DNA experiments.

β-Gal Staining, *in Situ* Hybridization, and Immunohistochemistry. Transgenic founder mice were established; subsequently, β-gal activity was analyzed in F1 hemizygous transgenic embryos according to the approach of Kimura *et al.* (11). *In situ* hybridization involving digoxygenin-labeled probes was conducted in a manner identical to that of Wilkinson (31). Whole-mount immunohistochemistry of anti-active-β-catenin (8E7; Upstate, Lake Placid, NY) was performed as described (8).

EMSA. The FOXA2 protein was produced employing an *in vitro* translational system (Promega, Madison, WI) as described (32). Binding reaction was conducted as reported (33). The competition assay included two molecular ratios of labeled oligonucleotides to unlabelled oligonucleotides, of 1:50 or 1:100. Oligonucleotides used for the assay were PE1-a (5′-GGTGTTATCAGCATTATTTATTTAGCCAAAGA), PE1-b (5′-GGGATTTCTTGAATTGTTTCTTTGTTTCTCAC), PE1-c (5′-GGAGGAGAGAAAGAGAAAAGAAAAACAGAAGG), and PE1-d (5′-GGGCAAAGGCATTTTGTCTTTTTATTCCCCT).

We are grateful to Drs. E. De Robertis (University of California, Los Angeles, CA), B. Hogan (Duke Unversity Medical Center, Durham, NC), H. Sasaki (RIKEN Center for Developmental Biology, Kobe, Japan), M. M. Shen (UMDNJ–Robert Wood Johnson Medical School, Piscataway, NJ), C. Niehrs (German Cancer Research Center, Heidelberg, Germany), B. G. Herrmann (Max-Planck-Institute for Molecular Genetics, Berlin, Germany), and H. Hamada (Osaka University, Suita, Japan) for plasmids. We also thank Mr. M. Suzuki of the Center for Animal Resources and Development (Kumamoto University) and Ms. R. Nakayama of LARGE (RIKEN CDB) for generating transgenic mice. This work was supported in part by grants-in-aid for Scientific Research on Priority Areas "Comparative Genomes" and (B) from the Ministry of Education, Culture, Sports, Science, and Technology of Japan and the Sumitomo Foundation. J.R. holds a Canadian Institutes of Health Research Distinguished Investigator award.

1. Beddington RS, Robertson EJ (1999) *Cell* 96:195–209.
2. Varlet I, Collignon J, Robertson EJ (1997) *Development (Cambridge, UK)* 124:1033–1044.
3. Thomas P, Beddington R (1996) *Curr Biol* 6:1487–1496.
4. Glinka A, Wu W, Delius H, Monaghan AP, Blumenstock C, Niehrs C (1998) *Nature* 391:357–362.
5. Piccolo S, Agius E, Leyns L, Bhattacharyya S, Grunz H, Bouwmeester T, De Robertis EM (1999) *Nature* 397:707–710.
6. Perea-Gomez A, Vella FD, Shawlot W, Oulad-Abdelghani M, Chazaud C, Meno C, Pfister V, Chen L, Robertson E, Hamada H, *et al.* (2002) *Dev Cell* 3:745–756.
7. Yamamoto M, Saijoh Y, Perea-Gomez A, Shawlot W, Behringer RR, Ang SL, Hamada H, Meno C (2004) *Nature* 428:387–392.
8. Kimura-Yoshida C, Nakano H, Okamura D, Nakao K, Yonemura S, Belo JA, Aizawa S, Matsui Y, Matsuo I (2005) *Dev Cell* 9:639–650.
9. Srinvas S (2006) *Genesis* 44:565–572.
10. Simeone A, Acampora D (2001) *Int J Dev Biol* 45:337–345.
11. Kimura C, Yoshinaga K, Tian E, Suzuki M, Aizawa S, Matsuo I (2000) *Dev Biol* 225:304–321.
12. Hardison RC (2000) *Trends Genet* 16:369–372.
13. Brenner S, Elgar G, Sandford R, Macrae A, Venkatesh B, Aparicio S (1993) *Nature* 366:265–268.
14. Kimura-Yoshida C, Kitajima K, Oda-Ishii I, Tian E, Suzuki M, Yamamoto M, Suzuki T, Kobayashi M, Aizawa S, Matsuo I (2004) *Development (Cambridge, UK)* 131:57–71.
15. Dufort D, Schwartz L, Harpal K, Rossant J (1998) *Development (Cambridge, UK)* 125:3015–3025.
16. Ang SL, Rossant J (1994) *Cell* 78:561–574.
17. Perea-Gomez A, Shawlot W, Sasaki H, Behringer RR, Ang S (1999) *Development (Cambridge, UK)* 126:4499–4511.
18. Wolfrum C, Besser D, Luca E, Stoffel M (2003) *Proc Natl Acad Sci USA* 100:11624–11629.
19. Jin O, Harpal K, Ang SL, Rossant J (2001) *Int J Dev Biol* 45:357–365.

20. Klingensmith J, Ang SL, Bachiller D, Rossant J (1999) *Dev Biol* 216:535–549.
21. Glinka A, Wu W, Onichtchouk D, Blumenstock C, Niehrs C (1997) *Nature* 389:517–519.
22. Piccolo S, Agius E, Leyns L, Bhattacharyya S, Grunz H, Bouwmeester T, DeRobertis EM (1999) *Nature* 397:707–710.
23. Mukhopadhyay M, Shtrom S, Rodriguez-Esteban C, Chen L, Tsukui T, Gomer L, Dorward DW, Glinka A, Grinberg A, Huang SP, *et al.* (2001) *Dev Cell* 1:423–434.
24. Olsen CL, Jeffery WR (1997) *Development (Cambridge, UK)* 124:3609–3619.
25. Taguchi S, Tagawa K, Humphreys T, Nishino A, Satoh N, Harada Y (2000) *Dev Genes Evol* 210:11–17.
26. Oda-Ishii I, Bertrand V, Matsuo I, Lemaire P, Saiga H (2005) *Development (Cambridge, UK)* 132:1663–1674.
27. Imai KS, Levine M, Satoh N, Satou Y (2006) *Science* 312:1183–1187.
28. Lamy C, Rothbacher U, Caillol D, Lemaire P (2006) *Development (Cambridge, UK)* 133:2835–2844.
29. Nagy A, Gertsenstein M, Vinterstein K, Behringer RR (2003) *Manipulating the Mouse Embryo* (Cold Spring Harbor Lab Press, Woodbury, NY).
30. Brault V, Moore R, Kutsch S, Ishibashi M, Rowitch DH, McMahon AP, Sommer L, Boussadia O, Kemler R (2001) *Development (Cambridge, UK)* 128:1253–1264.
31. Wilkinson DG (1998) *In Situ Hybridization* (Oxford Univ Press, New York).
32. Nakano T, Murata T, Matsuo I, Aizawa S (2000) *Biochem Biophys Res Commun* 267:64–70.
33. Foucher I, Montesinos ML, Volovitch M, Prochiantz A, Trembleau A (2003) *Development (Cambridge, UK)* 130:1867–1876.
34. Courtois V, Chatelain G, Han ZY, Le Novere N, Brun G, Lamonerie T (2003) *J Neurochem* 84:840–853.